Accepted Manuscript

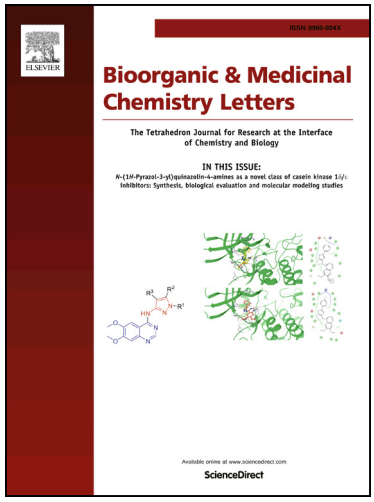

Pyrazole C-region Analogues of 2-(3-Fluoro-4-methylsulfonylaminophenyl)propanamides as Potent TRPV1 Antagonists

Sunho Lee, Changhoon Kim, Jihyae Ann, Shivaji A. Thorat, Eunhye Kim, Jongmi Park, Sun Choi, Peter M. Blumberg, Robert Frank-Foltyn, Gregor Bahrenberg, Hannelore Stockhausen, Thomas Christoph, Jeewoo Lee

PII: S0960-894X(17)30819-3
DOI: http://dx.doi.org/10.1016/j.bmcl.2017.08.020
Reference: BMCL 25214

To appear in: *Bioorganic & Medicinal Chemistry Letters*

Received Date: 4 July 2017
Revised Date: 8 August 2017
Accepted Date: 10 August 2017

Please cite this article as: Lee, S., Kim, C., Ann, J., Thorat, S.A., Kim, E., Park, J., Choi, S., Blumberg, P.M., Frank-Foltyn, R., Bahrenberg, G., Stockhausen, H., Christoph, T., Lee, J., Pyrazole C-region Analogues of 2-(3-Fluoro-4-methylsulfonylaminophenyl)propanamides as Potent TRPV1 Antagonists, *Bioorganic & Medicinal Chemistry Letters* (2017), doi: http://dx.doi.org/10.1016/j.bmcl.2017.08.020

Graphical Abstract

Pyrazole C-region Analogues of 2-(3-Fluoro-4-methyl sulfonylaminophenyl)propanamides as Potent TRPV1 Antagonists

Leave this area blank for abstract info.

Sunho Lee, Changhoon Kim, Jihyae Ann, Shivaji A. Thorat, Eunhye Kim, Jongmi Park, Sun Choi, Peter M. Blumberg, Robert Frank-Foltyn, Gregor Bahrenberg, Hannelore Stockhausen, Thomas Christoph, Jeewoo Lee*

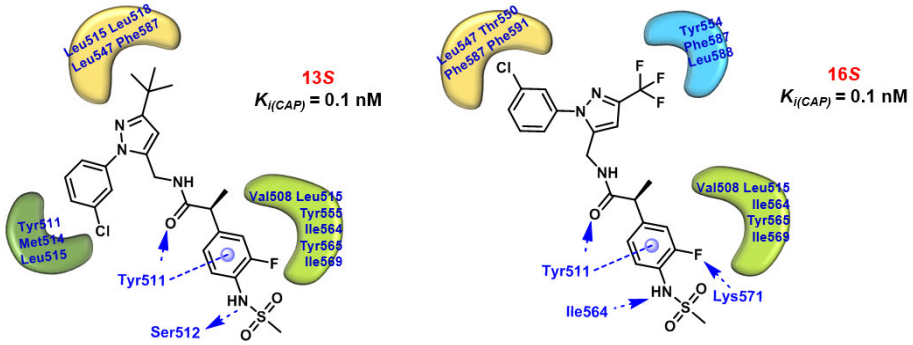

Bioorganic & Medicinal Chemistry Letters
journal homepage: www.elsevier.com

Pyrazole C-region Analogues of 2-(3-Fluoro-4-methylsulfonylaminophenyl)propanamides as Potent TRPV1 Antagonists

Sunho Lee [a], Changhoon Kim [a], Jihyae Ann [a], Shivaji A. Thorat [a], Eunhye Kim [b], Jongmi Park [b], Sun Choi [b], Peter M. Blumberg [c], Robert Frank-Foltyn [d], Gregor Bahrenberg [d], Hannelore Stockhausen [d], Thomas Christoph [d], Jeewoo Lee [a,*]

[a] *Laboratory of Medicinal Chemistry, Research Institute of Pharmaceutical Sciences, College of Pharmacy, Seoul National University, Seoul 08826, Korea*
[b] *National Leading Research Laboratory of Molecular Modeling & Drug Design, College of Pharmacy, Graduate School of Pharmaceutical Sciences, Ewha Womans University, Seoul 03760, Korea*
[c] *Laboratory of Cancer Biology and Genetics, Center for Cancer Research, National Cancer Institute, NIH, Bethesda, MD 20892, USA*
[d] *Grünenthal Innovation, Grünenthal GmbH, D-52078 Aachen, Germany*

ARTICLE INFO

Article history:
Received
Revised
Accepted
Available online

Keywords:
Vanilloid Receptor 1
TRPV1 Antagonist
Molecular Modeling

ABSTRACT

A series of 1-substituted 3-(*t*-butyl/trifluoromethyl)pyrazole C-region analogues of 2-(3-fluoro-4-methylsulfonamidophenyl)propanamides were investigated for *h*TRPV1 antagonism. The structure activity relationship indicated that the 3-chlorophenyl group at the 1-position of pyrazole was the optimized hydrophobic group for antagonistic potency and the activity was stereospecific to the *S*-configuration, providing exceptionally potent antagonists **13*S*** and **16*S*** with $K_{i(CAP)}$ = 0.1 nM. Particularly significant, **13*S*** exhibited antagonism selective for capsaicin and NADA and not for low pH or elevated temperature. Both compounds also proved to be very potent antagonists for *r*TRPV1, blocking *in vivo* the hypothermic action of capsaicin, consistent with their *in vitro* mechanism. The docking study of compounds **13*S*** and **16*S*** in our *h*TRPV1 homology model indicated that the binding modes differed somewhat, with that of **13*S*** more closely resembling that of **GRT12360**.

TRPV1, the target of capsaicin action, has emerged as a promising therapeutic target for the treatment of neuropathic pain and a range of other conditions, reflecting the central role of this nociceptor in the function of C-fiber sensory neurons.[1-3] Building on the demonstration of a receptor for capsaicin,[4] its cloning as TRPV1,[5] and insights arising from its structural analysis by cryo-EM[6,7] and homology modeling,[8,9] dramatic strides have been made in understanding the structure activity relations for antagonist binding to TRPV1.[10] These advances have been coupled with an appreciation of the complexity of TRPV1 regulation, such as the the finding that different antagonists may be differentially effective against different classes of TRPV1 activators such as capsaicin, low pH, or elevated temperature.[11] Such differences, in term, may translate into different physiological responses of animals or humans upon treatment with different TRPV1 antagonists.[12,13]

Over the past several years we have described an extensive series of *N*-(pyridin-3-ylmethyl) 2-(3-fluoro-4-(methylsulfon amido)phenyl)propanamides that showed potent and stereospecific human TRPV1 (*h*TRPV1) antagonism for multiple activators (**Figure 1**).[14-24] The pharmacophore of the antagonistic template (**Template I**) can be divided into the A, B and C-regions, analogous to the corresponding designation of regions for the agonist capsaicin. The structure activity relationships (SAR) of the template have been investigated in most detail for the pyridine C-region, in which a variety of functional groups including the amino, oxy, thio, alkyl, aryl and sulfonamido groups were incorporated at the 2-position of pyridine (R_2) along with substitution at the 6-position (R_1) with a trifluoromethyl[14-18,22] or *tert*-butyl group[24] as well as with the pyridine core modified by its isomers[19] or by a phenyl group.[21,24] In these studies, a number of compounds demonstrated highly potent antagonism toward TRPV1 activators including capsaicin (CAP), *N*-arachidonoyl dopamine (NADA), low pH, and heat (45 °C) and their antagonism were stereospecific to the *S*-configuration. Consistent with the *in vitro* mechanism of action of the compounds as *h*TRPV1 antagtonists, *in vivo* studies of selected potent antagonists indicated that these compounds blocked capsaicin-induced hypothermia and that they produced strong antiallodynic effects in neuropathic pain models. Docking studies

using our established *h*TRPV1 homology model[14] indicated that the 6-trifluoromethyl group and the 2-substituent in the pyridine C-region made hydrophobic interactions with pockets composed of Leu547/Thr550 and Met514/Leu515, respectively, that were critical for their potent antagonism.[14-18]

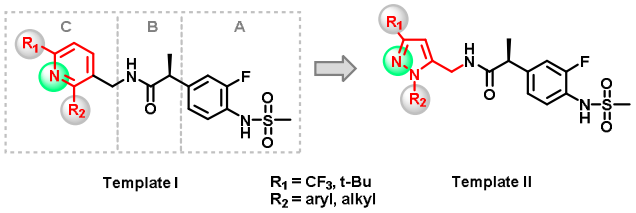

Figure 1. Design of pyrazole C-region TRPV1 antagonists

As part of our continuing effort to optimize TRPV1 antagonists as clinical candidates for neuropathic pain, we herein have investigated a series of pyrazole C-region derivatives of 2-(3-fluoro-4-methylsulfonylaminophenyl)propanamides (**Template II**) as a new antagonistic template. Since the pyrazole is a weak base and has a pyridine-like nitrogen (N2) with a lone electron pair, it serves as a bioisostere of pyridine. Furthermore, we anticipated that 1,3-substituents, R_1 and R_2, on pyrazole are better positioned to interact with the two hydrophobic pockets identified by the previous modeling than do the 2,6-substituents of pyridine.

In this paper, we synthesized a series of 1-substituted 3-(trifluoromethyl/*t*-butyl)pyrazole C-region derivatives and evaluated their antagonism toward activation of *h*TRPV1 by capsaicin. With selected potent antagonists in the series, we characterized in detail their *in vitro* activities and mode of action *in vivo*. Finally, we carried out a docking study using our *h*TRPV1 homology model to identify their mode of binding to the receptor.

N_1-Substituted 3-*t*-butyl-1H-pyrazole amines for the C-region were synthesized by one of two methods. In Method A, 4,4-dimethyl-3-oxopentanenitrile was condensed with different hydrazines to provide N_1-substituted 5-amino-3-*t*-butylpyrazoles whose amine was converted to the corresponding aminomethyl group in 3 steps to give the *t*-butylpyrazole C-region amine (**Scheme 1**). In Method B, *N*-Boc (3-*t*-butyl-pyrazol-5-yl)methanamine as a key intermediate for coupling with the corresponding boronic acids was prepared from 3,3-dimethylbutan-2-one in 6 steps. A Chan-Lam coupling reaction between pyrazole 1H-amine and aryl boronic acid followed by deprotection provided the *t*-butylpyrazole C-region amine (**Scheme 2**). N_1-Substituted 3-trifluoromethyl-1H-pyrazole amines for the C-region were synthesized from ethyl trifluoroacetic acid in 5 steps using different hydrazines (**Scheme 3**). A library of synthesized pyrazole C-region amines were coupled with 2-(3-fluoro-4-(methylsulfonamido)phenyl) propionic acids[14] to provide the final compounds.

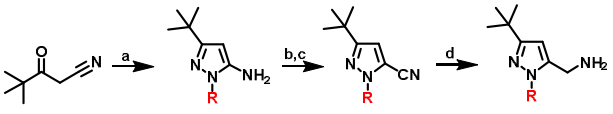

Scheme 1. Synthesis of 3-*t*-butyl pyrazole C-region (Method A). Reagents and conditions: (a) R-$NHNH_2$·HCl, EtOH:H_2O (1:1), reflux, overnight, 44-94%; (b) *t*-BuONO, CuI, CH_3CN, 0 °C to 65 °C; (c) $Zn(CN)_2$, $Pd(PPh_3)_4$, DMF, reflux, overnight; (d) $LiAlH_4$, THF, 0 °C to rt, 1 h, 12-26% (3 steps yield)

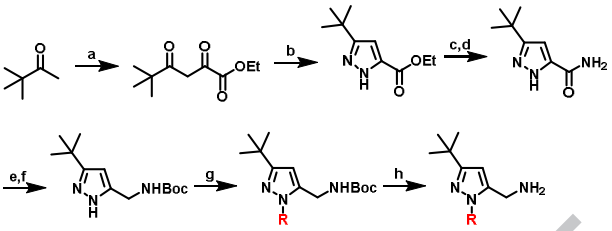

Scheme 2. Synthesis of 3-*t*-butyl pyrazole C-region (Method B). Reagents and conditions: (a) LiHMDS, diethyloxalate, THF, -78 °C to rt, overnight, 97%; (b) NH_2NH_2·2HCl, TEA, EtOH, rt, 2 h, 77%; (c) NaOH, MeOH:H_2O (5:1), rt, 2 h, 70%; (d) $SOCl_2$, MC, rt, overnight; then NH_4OH, MC, 0 °C, 1 h, 80%; (e) $LiAlH_4$, THF, 0 °C to rt, 3 h; (f) Boc_2O, MC, rt, 1 h, 50%; (g) Ar-$B(OH)_2$, $Cu(OAc)_2$, pyridine, MC, rt, 2 d; (h) TFA, MC, rt, overnight

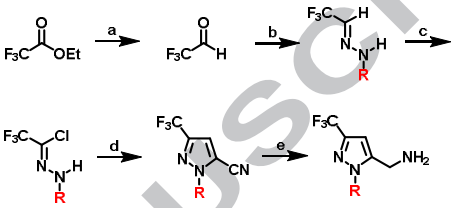

Scheme 3. Synthesis of 3-trifluoromethyl pyrazole C-region (Method C). Reagents and conditions: (a) $LiAlH_4$, Et_2O, -78 °C, 2 h; (b) R-$NHNH_2$, EtOH, reflux, 5 h, (**15**: 90%, **16**: 67%); (c) NCS, DMF, rt, (**15**: 48%, **16**: 26%); (d) 2-chloroacylonitrile, TEA, toluene, 80 °C, 20 h, (**15**: 44%, **16**: 80%); (e) $LiAlH_4$, THF, 0 °C to rt, 3 h, (**15**: 64%, **16**: 62%)

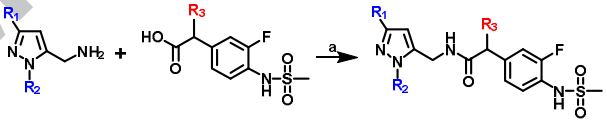

Scheme 4. General synthesis of 2-(3-fluoro-4-(methylsulfonamido)phenyl) propanamide analogues
Reagents and conditions: (a) EDC, HOBt, DMF, room temperature, 12 h.

The synthesized compounds were evaluated *in vitro* for TRPV1 antagonism as measured by inhibition of activation by capsaicin (100 nM). The assays were conducted using a fluorometric imaging plate reader (FLIPR) with *h*TRPV1 heterologously expressed in Chinese hamster ovary (CHO) cells.[14] The results are summarized in **Tables 1-3**.

First, we investigated the SAR of the N_1-substituent in the 3-*t*-butylpyrazole C-region (**Table 1**). The unsubstituted derivative (**1**) was found to be inactive, suggesting that the two hydrophobic groups were indispensable for activity by providing needed interactions with the receptor pockets as previously characterized for the pyridine C-region.[14-24] The incorporation of an alkyl group (**2**-**4**) enhanced the antagonism progressively as the size increased. The rigidity of alkyl groups further increased the potency (**3** *vs* **5**, **4** *vs* **6**). Most phenyl derivatives (**7**-**14**) showed potent antagonism. Among them, the 3-chlorophenyl derivative (**13**) displayed excellent antagonism with a $K_{i(CAP)}$ = 0.3 nM and its *S*-stereoisomer (**13*S***) exhibited a stereospecific activity with a $K_{i(CAP)}$ = 0.1 nM. The 4-fluoro-3-chlorophenyl derivatives (**14**, **14*S***) also showed high potency like those of the 3-chlorophenyl derivatives. The analysis of 4-substituted phenyl derivatives indicated that whereas the chloro group provided promising antagonism, electron-donating (**9**) and bulky (**11**,**12**) groups led to the dramatic reduction in activity.

Table 1. *In vitro h*TRPV1 antagonistic activities for 3-*t*-butylpyrazole derivatives

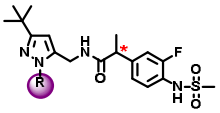

	R	$K_{i(CAP)}$ (nM)		R	$K_{i(CAP)}$ (nM)
1	H	NE	**9**	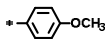	WE
2		WE	**10**		8.0
3		50.2	**11**		75.2
4		27.7	**12**	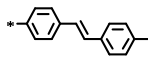	819
5		5.1	**13**		0.3
6		21.6	**13S**		0.1
7		8.0	**14**		0.5
8		3.7	**14S**		0.1

WE: weakly active, NE: not effective

Table 2. *In vitro h*TRPV1 antagonistic activities for 3-trifluoromethylpyrazole derivatives

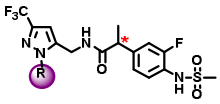

	R	$K_{i(CAP)}$ (nM)		R	$K_{i(CAP)}$ (nM)
15		0.4	**16**		0.3
15*S*		0.3	**16S**		0.1
15*R*		31.7	**16R**		26.5

Next, we explored the SAR of N_1-substituents in the 3-trifluoromethylpyrazole C-region (**Table 2**). Since 4- or 3-chlorophenyl derivatives in the 3-*t*-butylphenyl series provided the most promising activity, their surrogates were examined. 4-Chlorophenyl (**15**) and 3-chlorophenyl (**16**) derivatives displayed highly potent antagonism with $K_{i(CAP)}$ = 0.4 and 0.3 nM, respectively, in line with those of the 3-*t*-butylpyrazole series. In addition, the *S*-configuration was confirmed as the active configuration, as dramatically shown by isomers **15*S***, **16*S*** with $K_{i(CAP)}$ = 0.3 and 0.1 nM, versus isomers **15*R*, 16*R*** with $K_{i(CAP)}$ = 31.7 and 26.5 nM.

Finally, we investigated α-substituted acetamide B-region derivatives of the potent antagonist **13** (**Table 3**) because some of these B-region derivatives previously had provided high potency[20]. Unfortunately, they all displayed weak antagonism.

Table 3. *In vitro h*TRPV1 antagonistic activities for α-substituted acetamide derivatives

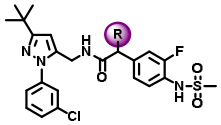

	R	$K_{i(CAP)}$ (nM)		R	$K_{i(CAP)}$ (nM)
17		WE	**19**		WE
18		WE			

WE: weakly active (**17**: 46%, **18**: 12%, **19**: 49% inhibition % at 5 μM)

Detailed *in vitro* activities of **13*S*** and **16*S***, the most potent antagonists in this series, were investigated for four different TRPV1 activators, *viz.* capsaicin, *N*-arachidonoyl dopamine (NADA), pH and heat (45°C), and compared to the activity of the previous lead **GRT12360** (**Table 4**). Both **13*S*** and **16*S*** showed excellent antagonism of *h*TRPV1 activation by capsaicin and NADA comparable to that of **GRT12360**. However, **13*S*** exhibited poor antagonism toward pH and heat, in contrast to **16*S*** and **GRT12360**, indicating that the size of the hydrophobic group at the 3-position in the pyrazole C-region affected the selectivity of antagonism for different activators.

Both antagonists proved to be highly potent antagonists of capsaicin action *in vivo* against rat TRPV1 (*r*TRPV1). Consistent with its *in vitro* mechanism of action ($K_{i(CAP)}$ = 0.1 nM in *r*/*h*TRPV1), they were able to block the acute hypothermic response to capsaicin (3 mg/kg, ip). The oral administration of 3 mg/kg **13*S*** and **16*S*** almost completely antagonized the effect of capsaicin on body temperature, with 95% and 85% inhibition, respectively, of the decrease in body temperature induced by capsaicin.

Table 4. Antagonistic activities of **13S** and**16S** for multiple activators in hTRPV1 and rTRPV1.

Activators, parameter	**13*S***	**16*S***	**GRT12360**[b]
***h*TRPV1**			
CAP (f)K_i (nM)	0.1	0.1	0.2
NADA (f)K_i (nM)	0.04	0.1	0.01
pH, IC_{50} (nM)	WE	8.0	6.3
heat 45°C, IC_{50} (nM)	WE	8.1	0.8
***r*TRPV1**			
CAP (f)K_i (nM)	0.1	0.1	
Anti-hypothermia	95%[a] at 3 mg/kg, po	85%[a] at 3 mg/kg, po	

[a] Inhibition percent to hypothermic response by 3 mg/kg ip capsaicin
[b] compound **49*S*** in ref 9

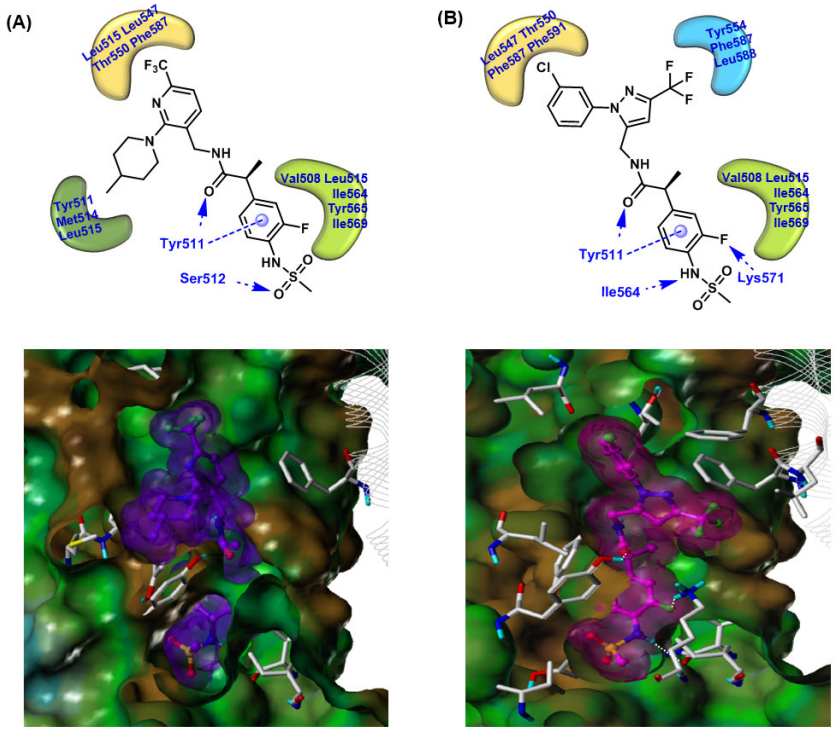

Figure 2. Binding modes of **GRT12360** and **16*S*** in the *h*TRPV1 model.[25]
(Top) 2-D representation of the binding interactions between **GRT12360** (A) and **16*S*** (B) with *h*TRPV1. Hydrogen bonding interactions are drawn in blue dashed line arrows, and hydrophobic interactions are displayed with curved patches. (Bottom) The Fast Connolly surface of *h*TRPV1 and the van der Waals surface of **GRT12360** and **16*S***. Using MOLCAD, the *h*TRPV1 molecular surface was created and the surface with the lipophilic potential property is presented. For clarity, the surface of *h*TRPV1 is Z-clipped and that of the ligands are colored individually by magenta and purple

In order to investigate the binding interactions of **13*S*** and **16*S***, flexible docking studies were carried out using our *h*TRPV1 model[14] constructed on the basis of our *r*TRPV1 model[8]. **13*S*** and **16*S*** share with the previously reported **GRT12360** (**Figure 2A**)[14] the identical A,B-region structure of 2-(3-fluoro-4-methylsulfonamidophenyl)propanamide but are distinguished by different C-regions. Compound **16*S*** has a 3-(trifluoromethyl)pyrazole ring and a chlorobenzene ring in the C-region and showed a different binding mode in the C-region compared to **GRT12360**. As shown in **Figure 2B**, the sulfonaminobenzyl group in the A-region occupied the deep bottom hole and participated in the hydrophobic interactions with Val508, Tyr511, Leu515, Ile564, Tyr565, and Ile569. In addition, the fluorine atom in the A-region engaged in hydrogen bonding with Lys571 while the NH of the sulfonamide group formed a hydrogen bond with Ile564. The amide group in B-region was able to form a hydrogen bond with Tyr511 and contributed to the proper positioning of the C-region for the hydrophobic interactions. In the C-region, the 3-(trifluoromethyl)pyrazole ring formed hydrophobic interactions with Tyr554 and with Phe587 and Leu588 of the adjacent monomer. Instead of the 3-(trifluoromethyl)pyrazole ring, the chlorobenzene ring oriented towards the upper hydrophobic region composed of Leu547, Thr550 and was involved in hydrophobic interactions with Phe587 and Phe591 in the adjacent monomer, which might have caused the flipped positioning of the two rings in the C-region.

On the other hand, **13*S***, which has the *t*-butyl pyrazole and chlorobenzene rings in the C-region, exhibited interactions similar to those of **GRT12360**[14]. As shown in **Figure 3A**, the 3-fluoro-4-methylsulfonamidophenyl group in the A-region bound well to the deep bottom area of the binding site, which consisted of Val508, Tyr511, Leu515, Tyr555, Ile564, Tyr565, and Ile569, forming hydrophobic interactions. Additionally, the NH of the sulfonamide group engaged in hydrogen bonding with Ser512. The amide group in the B-region made a hydrogen bond with the OH of Tyr511 and assisted the appropriate positioning of the C-region. The *t*-butyl pyrazole ring in the C-region extended toward the hydrophobic pocket composed of Leu515, Leu518, and Leu547, along with Phe587 from the adjacent monomer. Moreover, the chlorobenzene ring in the C-region participated in the hydrophobic interactions with Tyr511, Met514, and Leu515. Additionally, **13*S*** presented another comparable binding mode by flipping the two rings in the C-region as shown in **Figure 3B**. The 3-fluoro-4-methylsulfonamidophenyl group in the A-region fitted in the deep bottom region and showed hydrophobic interactions with Val508, Tyr511, Ile564, Tyr565, and Ile569. The NH of the amide group in the B-region formed a hydrogen bond with Asn551. Moreover, the *t*-butyl pyrazole ring in the C-region participated in hydrophobic interactions with Tyr511, Met514, and Leu515 as did the 4-methylpiperidine ring in **GRT12360**. The chlorobenzene ring approached the upper hydrophobic area, which included Leu518, Leu547, Thr550 and Phe587 from the adjacent monomer as did the 6-trifluoromethylpyridine ring in **GRT12360**.

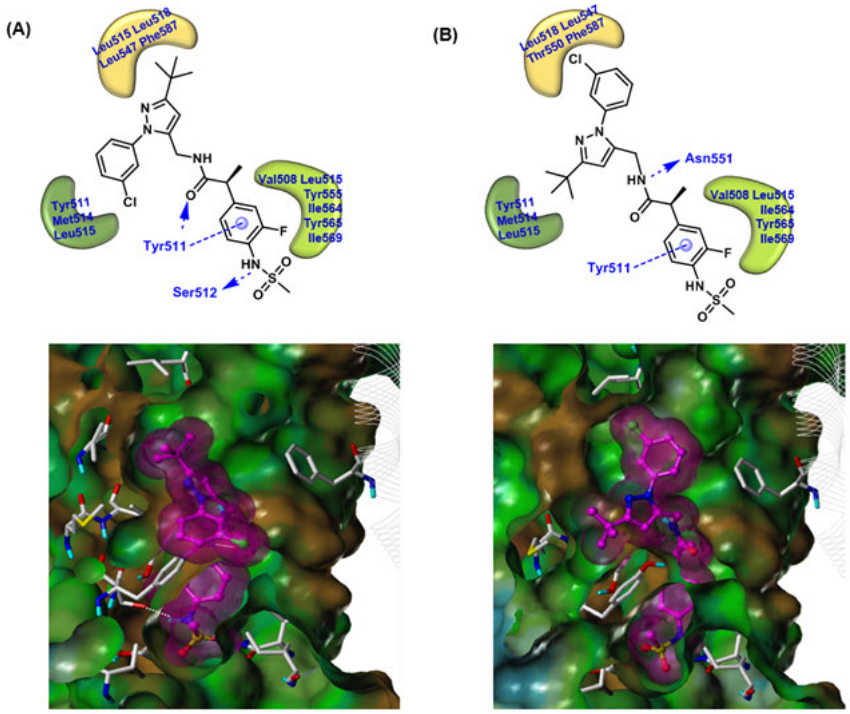

Figure 3. Binding modes of **13*S*** in the *h*TRPV1 model.[25]
(Top) 2-D illustrations of the two binding modes of **13*S*** with *h*TRPV1**.** Hydrogen bonding interactions are shown in blue dashed line arrows and hydrophobic interactions are presented with curved patches. (Bottom) The Fast Connolly surface representation of *h*TRPV1 and the van der Waals surface representation of the ligand **13*S***. MOLCAD was used to generate the molecular surface of *h*TRPV1 and the surface is displayed with the lipophilic potential property. For clarity, the surface of *h*TRPV1 is Z-clipped and that of **13*S*** is in magenta color.

In summary, the structure activity relationship of 3-(*t*-butyl)pyrazole and 3-(trifluoromethyl)pyrazole C-region derivatives of 2-(3-fluoro-4-methylsulfonamidophenyl) propanamides as antagonists for *h*TRPV1 was investigated. The 3-chlorophenyl group at the 1-position of pyrazole was the optimal hydrophobic group for antagonism and the activity was stereospecific for the *S*-configuration, providing the exceptionally potent antagonists **13*S*** and **16*S*** with $K_{i(CAP)}$ = 0.1 nM. Whereas **16*S*** showed full antagonism to all activators as did the previous lead, **13*S*** exhibited antagonism selective for capsaicin and NADA but not low pH or elevated temperature. Both compounds also proved to be very potent antagonists for *r*TRPV1 and blocked the hypothermic effect of capsaicin *in vivo*, consistent with their *in vitro* mechanism. The docking study of compounds **13*S*** and **16*S*** in our *h*TRPV1 homology model indicated that they displayed different binding interactions and that the mode of **13*S*** was more like that of **GRT12360**.

Acknowledgments
This research was supported by research grants from Grünenthal in Germany, a grant from the National Research Foundation (NRF) of Korea (NRF-2016M3A9B5939892), a grant from the Mid-career Researcher Program (NRF-2017R1A2B4010084) funded by the Ministry of Science, ICT and Future Planning (MSIP) and the NRF, and in part by the Intramural Research Program of the National Institutes of Health, Center for Cancer Research, National Cancer Institute (Project Z1A BC 005270) in the USA.

References and Notes

1. Szallasi, A.; Blumberg, P. M. *Pharmacol. Rev*. **1999**, 51, 159.
2. Tominaga, M.; Caterina, M. J.; Malmberg, A. B.; Rosen, T. A.; Gilbert, H.; Skinner, K.; Raumann, B. E.; Basbaum, A. I.; Julius, D. *Neuron* **1998**, 21, 531.
3. Cui, M.; Gosu, V.; Basith, S.; Hong, S.; Choi, S. *Adv Protein Chem. Struct. Biol.* **2016**, 104, 81.
4. Szallasi, A.; Blumberg, P.M. *Brain Res*. **1990**, 524, 106.
5. Caterina, M.J.; Schumacher, M.A.; Tominaga, M.; Rosen, T.A.; Levine, J.D.; Julius, D. *Nature* **1997**, 389, 816.
6. Liao, M.; Cao, E.; Julius, D.; Cheng, Y. *Nature* **2013**, 504, 107.
7. Cao, E.; Liao, M., Cheng, Y.; Julius, D. *Nature* **2013**, 504, 113.
8. Lee, J. H.; Lee, Y.; Ryu, H.; Kang, D. W.; Lee, J.; Lazar, J.; Pearce, L. V; Pavlyukovets, V. A.; Blumberg, P. M.; Choi, S. *J. Comput. Aided Mol. Des.* **2011**, 25, 317.
9. Feng, Z.; Pearce, L.V.; Xu, X.; Yang, X.; Yang, P.; Blumberg, P.M.; Xie, X.Q. *J. Chem. Inf. Model*. **2015**, 55, 572.
10. (a) Kym, P. R.; Kort, M. E.; Hutchins, C. W. *Biochem. Pharmacol*. **2009**, 78, 211. (b) Wong, G. Y.; Gavva, N. R. *Brain Res. Rev*. **2009**, 60, 267. (c) Gunthorpe, M. J.; Chizh, B. A. *Drug Disc. Today* **2009**, 14, 56. (d) Lazar, J.; Gharat, L.; Khairathkar-Joshi, N.; Blumberg, P. M.; Szallasi, A. *Exp. Opin. Drug Discov.* **2009**, 4, 159. (e) Voight, E. A.; Kort, M. E. *Exp. Opin. Ther. Pat.* **2010**, 20, 1. (f) Szolcsányi, J.; Sándor, Z. *Trend Pharmacol. Sci.* **2012**, 33, 646. (g) Szallasi, A.; Sheta, M. *Exp. Opin. Investig. Drug* **2012**, 21, 1351. (h) De Petrocellis L.; Moriello A. S. *Recent Patents on CNS Drug Discovery* **2013**, 8, 180. (i) Lee, Y.; Hong, S.; Cui, M.; Sharma, P. K. Lee, J.; Choi, S. *Exp. Opin. Ther. Pat*. **2015**, 25, 291. (j) Tabrizi, M. A.; Baraldi, P. G.; Baraldi, S.; Gessi, S.; Merighi, S.; Borea, P. A. *Med. Res. Rev*. **2017**, 37, 936.

11. Reilly, R. M.; McDonald, H. A.; Puttfarcken, P. S.; Joshi, S. K.; Lewis, L.; Pai, M.; Franklin, P. H.; Segreti, J. A.; Neelands, T. R.; Han, P.; Chen, J.; Mantyh, P. W.; Ghilardi, J. R.; Turner, T. M.; Voight, E. A.; Daanen, J. F.; Schmidt, R. G.; Gomtsyan, A.; Kort, M. E.; Faltynek, C. R.; Kym, P. R. *J. Pharm. Exp. Ther* . **2012**, 342, 416.
12. Gomtsyan, A.; McDonald, H. A.; Schmidt, R. G.; Daanen, J. F.; Voight, E. A.; Segreti, J. A.; Puttfarcken, P. S.; Reilly, R. M; Kort, M. E.; Dart, M. J.; Kym, P. R. *Temperature (Austin)* **2015**, 2, 297.
13. Garami, A.; Shimansky, Y. P.; Pakai, E.; Oliveira, D. F., Gavva, N. R.; Romanovsky, A. A. *J. Neurosci.* **2010**, 30, 1435.
14. Kim, M. S.; Ryu, H.; Kang, D. W.; Cho, S-H.; Seo, S.; Park, Y. S.; Kim, M-Y.; Kwak, E. J.; Kim, Y. S.; Bhondwe, R. S.; Kim, H. S.; Park, S-g. Son, K.; Choi, S.; DeAndrea-Lazarus, I.; Pearce, L. V.; Blumberg, P. M.; Frank, R.; Bahrenberg, G.; Stockhausen, H.; Kögel, B. Y.; Schiene, K.; Christoph, T.; Lee, J. *J. Med. Chem.* **2012**, 55, 8392.
15. Thorat, S. A.; Kang, D. W.; Ryu, H.; Kim, M. S.; Kim, H. S.; Ann, J.; Ha, T-H.; Kim, S. E.; Son, K.; Choi, S.; Blumberg, P. M.; Frank, R.; Bahrenberg, G.; Schiene, K.; Christoph, T.; Lee, J. *Eur. J. Med. Chem.* **2013**, 64, 589.
16. Ha, T-H; Ryu, H.; Kim, S-E.; Kim, H. S.; Ann, J.; Tran, P-T.; Hoang, V-H.; Son, K.; Cui, M.; Choi, S.; Blumberg, P. M.; Frank, R.; Bahrenberg, G.; Schiene, K.; Christoph, T.; Frormann, S.; Lee, J. *Bioorg. Med. Chem.* **2013**, 21, 6657.
17. Ryu, H.; Seo, S.; Cho, S-H.; Kim, H. S.; Jung, A.; Kang, D. W.; Son, K.; Cui, M.; Hong, S-h.; Sharma, P. K.; Choi, S.; Blumberg, P. M.; Frank-Foltyn, R.; Bahrenberg, G.; Stockhausen, H.; Schiene, K.; Christoph, T,; Frormann, S.; Lee, J. *Bioorg. Med. Chem. Lett.* **2014**, 24, 4039.
18. Ryu, H.; Seo, S.; Cho, S-H.; Kim, M. S.; Kim, M-Y.; Kim, H. S.; Ann, J.; Tran, P-T.; Hoang, V-H,; Byun, J.; Cui, M.; Son, K.; Sharma, P. K.; Choi, S.; Blumberg, P. M.; Frank-Foltyn, R.; Bahrenberg, G.; Koegel, B-Y.; Christoph, T.; Frormann, S.; Lee, J. *Bioorg. Med. Chem. Lett.* **2014**, 24, 4044.
19. Ryu, H.; Seo, S.; Lee, J-Y.; Ha, T-H.; Lee, S.; Jung, A.; Ann, J.; Kim, S-E.; Yoon, S.; Hong, M.; Blumberg, P. M.; Frank-Foltyn, R.; Bahrenberg, G.; Schiene, K.; Stockhausen, H.; Christoph, T.; Frormann, S.; Lee, J. *Eur. J. Med. Chem.* **2015**, 93, 101.
20. Tran, P-T. Kim, H. S.; Ann, J.; Kim, S-E.; Kim, C.; Hong, M.; Hoang, V-H.; Ngo, V. T. H.; Hong, S.; Cui, M.; Choi, S.; Blumberg, P. M.; Frank-Foltyn, R.; Bahrenberg, G.; Stockhausen, H.; Christoph, T.; Lee, J. *Bioorg. Med. Chem. Lett.* **2015**, 25, 2326.
21. Ann, J.; Jung, A.; Kim, M-Y.; Kim, H-M.; Ryu. H.; Kim, S.; Kang, D. W.; Hong, S.; Cui, M.; Choi, S.; Blumberg, P. M.; Frank-Foltyn, R.; Bahrenberg, G.; Stockhausen, H.; Christoph, T.; Lee, J. *Bioorg. Med. Chem.* **2015**, 23, 6844.
22. Ann, J.; Ki, Y.; Yoon, S.; Kim, M. S.; Lee, J-U.; Kim, C.; Lee, S.; Jung, A.; Baek, J.; Hong, S.; Choi, S.; Pearce, L. V.; Esch, T.; Turcios, N. A.; Lewin, N. E.; Ogunjirin, A. E.; Herold, B. K. A.; McCall, A. K.; Blumberg, P. M.; Lee, J. *Bioorg. Med. Chem.* **2016**, 24, 1231.
23. Ann, J.; Sun, W.; Zhou, X.; Jung, A.; Baek, J.; Lee, S.; Kim, C.; Yoon, S.; Hong, S.; Choi, S.; Turcios, N. A.; Herold, B. K. A.; Esch, T. E.; Lewin, N. E.; Abramovitz, A.; Pearce, L. V.; Blumberg, P. M. Lee, J. *Bioorg. Med. Chem. Lett.* **2016**, 26, 3603.
24. Lee, S.; Kang, D. W.; Ryu, H.; Kim, C.; Ann, J.; Lee, H.; Kim, E.; Hong, S.; Choi, S.; Blumberg, P. M.; Frank-Foltyn, R.; Bahrenberg, G.; Stockhausen, H.; Christoph, T.; Lee, J. *Bioorg. Med. Chem.* **2017**, 25, 2451.
25. The 3D structures of the **13*S*** and **16*S*** were generated using Concord and energy minimized with MMFF94s force field and MMFF94 charge until the rms of Powell gradient was 0.05 kcal $mol^{-1}A^{-1}$ in SYBYL-X 2.0 (Tripos Int., St. Louis, MO, USA). The flexible docking study on our *h*TRPV1 model was carried out using GOLD v.5.2 (Cambridge Crystallographic Data Centre, Cambridge, UK), which employes a genetic algorithm (GA) and allows for full ligand flexibility and partial protein flexibility. The binding site was defined as 8 Å around the capsaicin docked in the *h*TRPV1 model. The important side chains of the nine residues (i.e., Tyr511, Ser512, Met514, Leu515, Leu518, Phe543, Leu547, Thr550, and Asn551) were set to be flexible with 'crystal mode' in GOLD. **13*S*** and **16*S*** was docked with the GoldScore scoring function with 30 GA runs, and the other parameters were remainded as default. All the computation calculations were undertaken on an Intel® Xeon™ Quad-core 2.5 GHz workstation with Linux Cent OS release 5.5.